Journal of Thermal Biology 49-50 (2015) 74–81

Contents lists available at ScienceDirect

Journal of Thermal Biology

journal homepage: www.elsevier.com/locate/jtherbio

A comparative study of thermal effects of 3 types of laser in eye: 3D simulation with bioheat equation

Amin Joukar [a], Erfan Nammakie [a], Hanieh Niroomand-Oscuii [b,*]

[a] Mechanical Engineering Faculty, Sahand University of Technology, Sahand New Town, Tabriz, Iran
[b] Mechanical Engineering Faculty, Sahand University of Technology, P.O. Box: 51335-1996, Sahand New Town, Tabriz, Iran

ARTICLE INFO

Article history:
Received 2 October 2014
Received in revised form
10 February 2015
Accepted 10 February 2015
Available online 13 February 2015

Keywords:
Pennes bioheat equation
Blood perfusion
Nd:Yag laser
Nd:Yap laser
Argon laser

ABSTRACT

The application of laser in ophthalmology and eye surgery is so widespread that hardly can anyone deny its importance. On the other hand, since the human eye is an organ susceptible to external factors such as heat waves, laser radiation rapidly increases the temperature of the eye and therefore the study of temperature distribution inside the eye under laser irradiation is crucial; but the use of experimental and invasive methods for measuring the temperature inside the eye is typically high-risk and hazardous. In this paper, using the three-dimensional finite element method, the distribution of heat transfer inside the eye under transient condition was studied through three different lasers named Nd:Yag, Nd:Yap and ArF. Considering the metabolic heat and blood perfusion rate in various regions of the eye, numerical solution of space–time dependant Pennes bioheat transfer equation has been applied in this study. Lambert–Beer's law has been used to model the absorption of laser energy inside the eye tissues. It should also be mentioned that the effect of the ambient temperature, tear evaporation rate, laser power and the pupil diameter on the temperature distribution have been studied. Also, temperature distribution inside the eye after applying each laser and temperature variations of six optional regions as functions of time have been investigated. The results show that these radiations cause temperature rise in various regions, which will in turn causes serious damages to the eye tissues. Investigating the temperature distribution inside the eye under the laser irradiation can be a useful tool to study and predict the thermal effects of laser radiation on the human eye and evaluate the risk involved in performing laser surgery.

1. Introduction

Since the invention of the first laser by Maiman in 1960, researchers have studied the miscellaneous applications of lasers in various fields. Laser surgery is definitely one the most important of these applications which is regarded as one of the most significant developments in the medicine of the present century. In fact, it can be claimed that different types of lasers have been proposed as unrivalled tools in modern medicine.

Laser systems have been divided into two categories: continuous wave lasers and pulsed lasers. Most gas lasers and some solid-state lasers belong to the first group, whereas pulsed lasers family mainly include dye lasers.

Medical lasers have important parameters. The time duration of laser radiation is a serious parameter for the interaction of laser with biological tissue. The second important parameter is the wavelength of the laser which defines the penetration depth of the laser into the tissue. The third parameter, which is the density of laser energy, is also significant. The fourth parameter that should be taken into account is the intensity of radiation, which by definition is the ratio of energy density to the pulse width.

Today, a variety of lasers are used to treat and diagnose diseases in ophthalmology. Since the use of laser in treatment of retinal detachment disease, this type of surgery is known as a common approach. Other applications of laser in this field include glaucoma and cataracts treatment (Niemz, 2007).

Numerical simulation of laser irradiation is a fast and easy assessment to predict the temperature distribution in the eye without the need for invasive tests. Taflove and Brodwin (1975) showed temperature distribution in the eye by a finite difference model. Using Pennes bioheat equation and invasive tests, Priebe et al. (1975) and Emery et al. (1975) proposed one of the first these computer models for temperature distribution inside rabbit eye. Lagendijk (1982) presented different mathematical eye models for

* Corresponding author. Fax: +98-41-33459494.
E-mail addresses: a_joukar@sut.ac.ir (A. Joukar), e_nammakie@sut.ac.ir (E. Nammakie).

http://dx.doi.org/10.1016/j.jtherbio.2015.02.004
0306-4565/

humans and rabbits in 1982 before Scott developed a FEM-model of the human eye in 1988. Based on these works, many different eye models have been developed until today. Ng and Ooi (2006) solved the temperature distribution inside the eye under steady state condition. In his model, three layers of retina, sclera and choroid were considered as a single layer. In previous works mentioned earlier, the effect of laser on the eye tissue was not investigated and the models only included the simplifying of the eye. On the other hand, numerical simulation of laser surgery has been performed by various scientists. Applying finite volume method, Narasimhan et al. (2010) numerically studied the two-dimensional transient heat transfer in laser surgery. Taking into account all the layers of the eye, the blood perfusion and metabolic heat in ciliary body and retina, Cvetković et al. (2008) analysed the effect of the Nd:Yag laser for the surgery of cornea. In his model, the effect of the blood perfusion and metabolic heat inside the choroid was not considered. Mirnezami et al. (2013) used his model to assess the irradiation of the whole eye, using only the scleral heat transfer and they did not consider all parts of eye in their model. Heussner et al. (2014) presented a three-dimensional thermo-dynamic model of the human eye for the prediction of temperatures and damage thresholds under irradiation and they consider blood flow in their simulation.

In this paper, the distribution of heat transfer inside the eye under transient condition was studied through three different lasers and the effect of the ambient temperature, tear evaporation rate, laser power and the pupil diameter on the temperature distribution have been studied. Finally, temperature distribution inside the eye after applying each laser and temperature variations of six optional regions as functions of time have been investigated.

2. Theoretical background

2.1. Anatomy

The eye is not shaped like a perfect sphere, rather it is a fused two-piece unit. The smaller frontal unit, more curved, called the cornea is linked to the larger unit called the sclera. Light enters the cornea from outside and after passing through the pupil reaches the lens. The lens focuses light precisely on the retina so that a clear image on the retina is created. Irradiation targets in laser treatment divide the eye into two anterior and posterior parts. The anterior part of the eye includes the cornea, iris and the ciliary body, while the posterior part of the eye is composed of lens, vitreous and retina. A schematic of the human eye can be seen in Fig. 1. (Niemz, 2007).

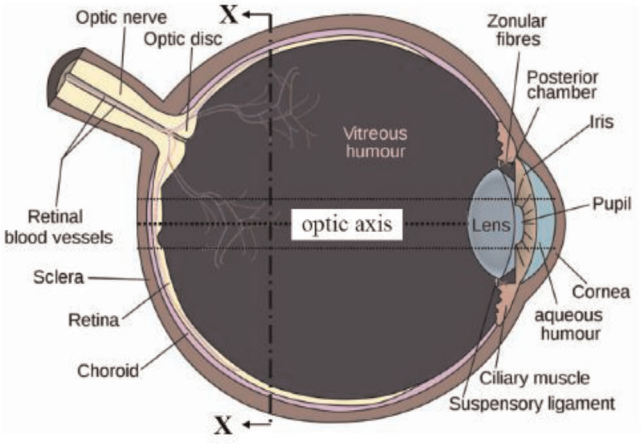

Fig. 1. A schematic of the human eye (Narasimhan et al., 2010).

2.2. Governing equations

2.2.1. Heat transfer equations

The governing equation in this simulation is the Pennes bioheat equation and its general form is as follows (Pennes, 1948).

$$\rho C_p \frac{\partial T}{\partial t} + \rho C_p u \cdot \nabla T = \nabla \cdot (k \nabla T) + Q + \rho_b C_b \omega_b (T_b - T) + Q_{met} \quad (1)$$

In this equation $\rho$is density, C_p is the specific heat, ω_b is the rate of blood perfusion, k is the thermal conductivity and Q_{met} is the metabolic flux. These values for each tissue can be seen in Table 1. Moreover, T_b is the blood temperature, C_b is the specific heat of blood and ρ_b is the density of blood which are equal to 37 °C, 3594 J/kg °C and 1060 kg/m^3, respectively.

Pennes bioheat equation is used due to the presence of blood perfusion and metabolic heat flux terms in this equation.

2.2.2. Laser equations

When modelling the laser source, one can use a simplifying fact that many laser beams are of a Gaussian profile. This consideration is valid when the beam divergence is very small as is the case for a laser. Thus, the solutions for the the intensity can be represented in the form of a Gaussian function. Beer–Lambert equation is used for applying the effect of laser. Energy density ($Q(r,z,t)$) absorbed by the tissues of the eye is defined using the following equation (Narasimhan and Jha, 2012).

$$Q(r, z, t) = \alpha I(r, z, t) \quad (2)$$

Where α is the laser wavelength, which depends on the absorption coefficient of the tissue. Absorption coefficients of each tissue are shown in Table 2 for all three lasers.

In Eq. (2), I is the intensity of the Laser which is defined as follows (Narasimhan and Jha, 2012).

$$I(r, z, t) = I_0 \exp\left(-\frac{2r^2}{w^2} - \alpha z\right) \exp\left(-\frac{8t^2}{\tau^2}\right) \quad (3)$$

In this equation, I_0 is the initial intensity of the laser, w is the diameter of the laser (0.5 mm) and τ is the pulse duration of the laser which are equal to 100 ns, 10 ms and 1 ms for Argon, Nd:Yag and Nd:Yap lasers, respectively. The most crucial characteristic of the eye tissues is the absorption coefficient resulting from its drastic dependence on the wavelength of the laser. Therefore, for different tissues of the eye, the absorption occurs at specific wavelengths.

3. Material and methods

In this paper, we used the three-dimensional finite element method, the distribution of heat transfer inside the eye under transient condition was studied through three different lasers named Neodymium-Doped Yttrium Aluminium Garnet (Nd:Yag), Neodymium-Doped Yttrium Aluminium Perovskite (Nd:Yap)and Argon Fluoride (ArF)with wavelengths of 1340, 1064 and 193 nm, respectively. Considering the metabolic heat and blood perfusion rate in various regions of the eye, numerical solution of space–time dependant Pennes bioheat transfer equation has been applied in this study. Lambert–Beer's law has been used to model the absorption of laser energy inside the eye tissues. It should also be mentioned that the effect of the ambient temperature, tear evaporation rate, laser power and the pupil diameter on the temperature distribution have been studied. Finally, temperature distribution inside the eye after applying each laser and temperature variations of six optional regions as functions of time have been investigated.

Table 1
Characteristics of different tissues of the eye, (Gokul et al., 2013; DeMarco et al., 2003)

Tissue	Rate of blood perfusion (1/s)	Metabolic flux (W/m^3)	Thermal conductivity (W/m °C)	Specific heat (J/kg °C)	Density (kg/m^3)
Vitreous humour	0	0	0.594	3997	1000
Lens	0	0	0.4	3000	1050
Aqueous humour	0	0	0.578	3997	996
Cornea	0	0	0.580	4178	1050
Sclera	0	0	0.58	4178	1100
Iris	0.0027	690	0.498	3340	1100
Choroid	0.021	1000	0.53	3840	1100
Retina	0.035	10000	0.565	3680	992

Table 2
Absorption coefficients of each tissue and laser parameters, (Cvetković et al., 2008; Jelinkova et al., 2004)

	Ar laser (193 nm)	Nd:Yag laser (1064 nm)	Nd:Yap laser (1340 nm)
Vitreous humour	542.7	20	224
Lens	2558	43.5	235
Aqueous humour	2228	35	222
Cornea	270000	113	240
Sclera	28800	634.8	340
Iris	2228	42.5	222
Choroid	48475	6615	222
Retina	6526	10000	1150
Wave Length	193 nm	1064 nm	1340 nm
Pulse Duration	140 ns	10 ms	1 ms
w(Beam Diameter of Laser)		0.5 mm	
Laser Power		0.1, 0.15, 0.2 W	

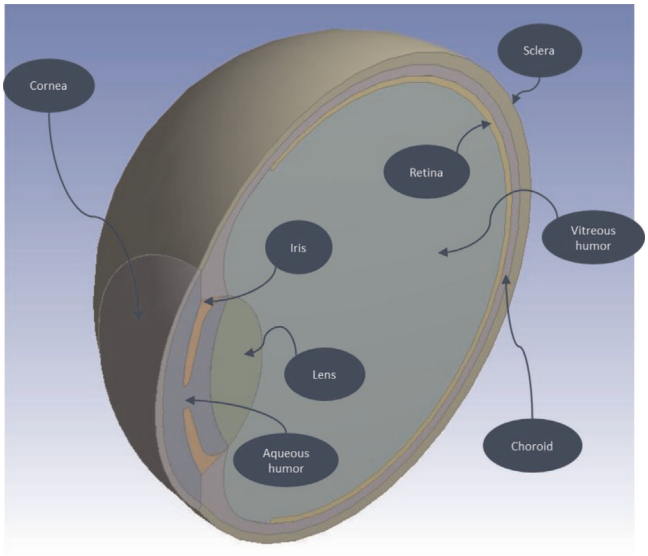

Fig. 2. Different parts of human eye anatomy in three dimensions.

3.1. Geometry

The model considered for the present paper and its dimensions are shown in : Fig. 2 and Table 3, respectively. As can be seen in the this figure, the three-dimensional model consists of eight different layers of the eye containing the aqueous humour, lens, vitreous, cornea, sclera, iris, retina and choroid. In some laser modelling (Chua et al., 2005; Ooi et al., 2007; Jelinkova et al., 2004), the retina and the choroid layers have been considered as a homogeneous layer with sclera. However, studies suggest a dramatic difference among these three layers in terms of absorption coefficient. Therefore, in order to increase the accuracy of modelling, each of these layers has been separately simulated and also their

Table 3
Geometrical values used in this work, (Ng and Ooi, 2006; Narasimhan et al., 2010)

Tissue	Parameter (mm)
Cornea	Thickness: 0.6 Height: 12
Lens	Thickness: 4 Height: 10.5
Aqueous humour	Length: 3.5
Iris	Thickness: 0.35
Vitreous humour	Length: 16.5
Retina	Thickness: 0.2
Choroid	Thickness: 0.3
Sclera	Thickness: 0.5 Height: 22

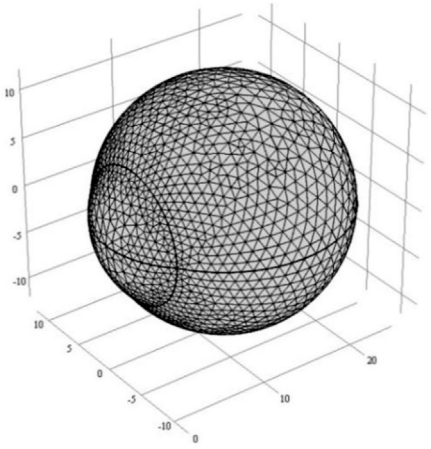

Fig. 3. Tetrahedral mesh for various parts of eye anatomy.

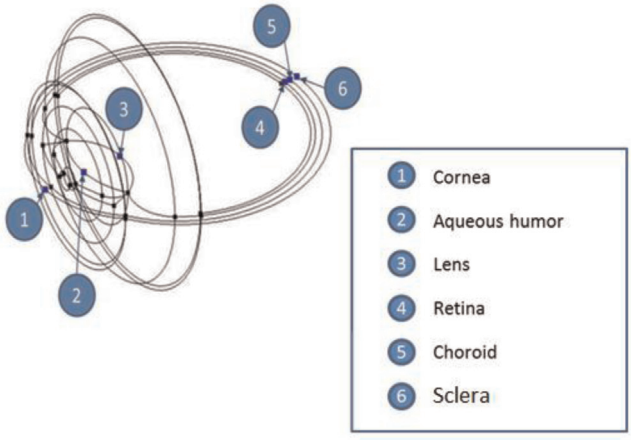

Fig. 4. Optional points (cornea, aqueous humour, lens, retina, choroid, sclera) for temperature distribution analysis.

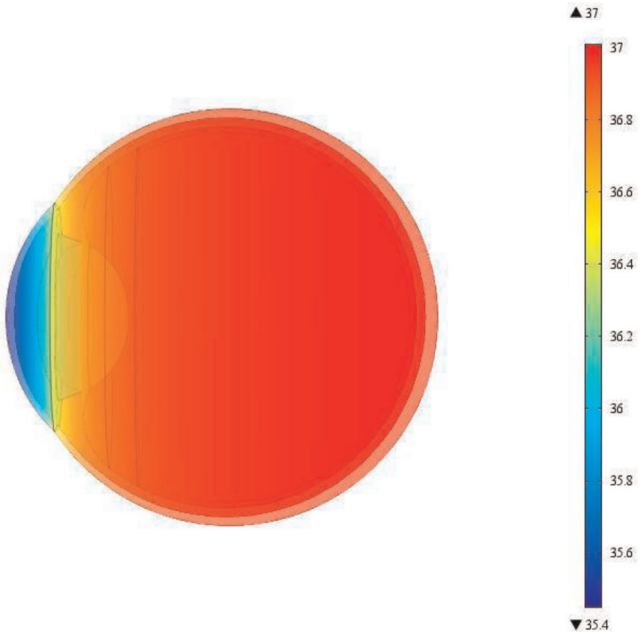

Fig. 5. Temperature distribution inside the eye under steady conditions by taking the values of Table 1.

absorption coefficients have been defined individually.

Using Comsol 4.4 software, finite element method has been applied in this simulation. Mesh generation of the model is depicted in Fig. 3 and 109907 tetrahedral elements have been used.

3.2. Boundary conditions

Boundary conditions are defined as follows:

1. In the back of the eye, heat is transferred from the blood in the arteries of the retina to the sclera:

$$k\frac{\partial T}{\partial n} = h_{bl}(T - T_{bl}) \tag{4}$$

In the above equation, n is the normal direction to the boundary surface, h_{bl} is the heat transfer coefficient between the blood and the eye (65 W/m^2 K) and T_{bl} is the temperature of the blood (37 °C).

2. In cornea, heat loss occurs through convection, radiation and evaporation of tear;

$$k\frac{\partial T}{\partial n} = h_{amb}(T - T_{amb}) + \sigma\varepsilon\left(T^4 - T_{amb}^4\right) + E \tag{5}$$

In this equation, h_{amb} is the heat transfer coefficient between the eye and air, T_{amb} is the ambient temperature (25 °C), σ is the Stefan–Boltzmann constant (5.67E−08 W/m^2 K^4), ε is the emissivity of the retina and E is the tear evaporation rate of the eye (40 W/m^2) (Scott, 1988; Gokul et al., 2013).

4. Results

In this section, the effect of the lasers mentioned earlier on the designed model will be discussed separately. First, we will present the temperature distributions under steady conditions. The obtained results then will be used as the initial conditions for the transient solutions. Meanwhile, the temperature variations of the six optional points on the central axis of the eye (Fig. 4) at the exposure time of the lasers and shortly thereafter will be discussed, separately. In addition to this, the effects of important parameters such as the diameter of pupillary opening and power of laser will be studied.

4.1. Steady state condition results

Temperature distribution under steady conditions is presented in Fig. 5. Furthermore, the temperature distributions along the pupillary axis for four various ambient temperatures (cold to warm) and four different tear evaporation rates are shown in Figs. 6 and 8. Fig. 7 shows that how temperature distribution under ambient temperature of 25 °C obtained from our results is validated with other works.

4.2. Transient condition results

The results of the steady state solutions will now be used as the initial conditions for applying three different lasers under transient conditions.

Nd:Yag laser: Fig. 9 presents the temperature distribution inside the eye after applying this laser. The temperature variations of six optional points can be seen in Fig. 10 The effects of the pupil diameter and the laser power on the temperature of retina are also so pivotal which can be hardly neglected. These effects have been depicted in Figs. 11 and 12 respectively.

Nd:Yap laser: Fig. 13 shows the temperature distribution inside the eye after applying this laser. Moreover, Fig. 14 indicates the

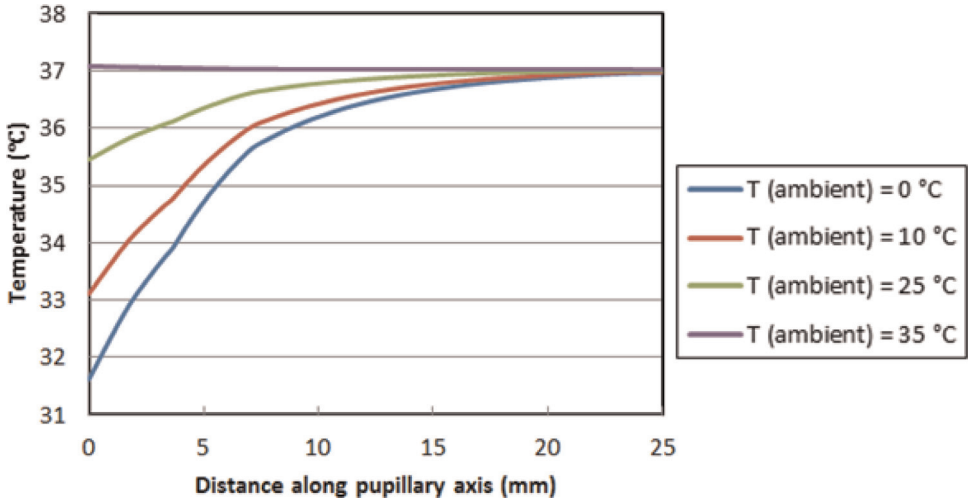

Fig. 6. Temperature distribution under steady condition for four different ambient temperatures (0, 10, 25 and 35 °C) along pupillary axis.

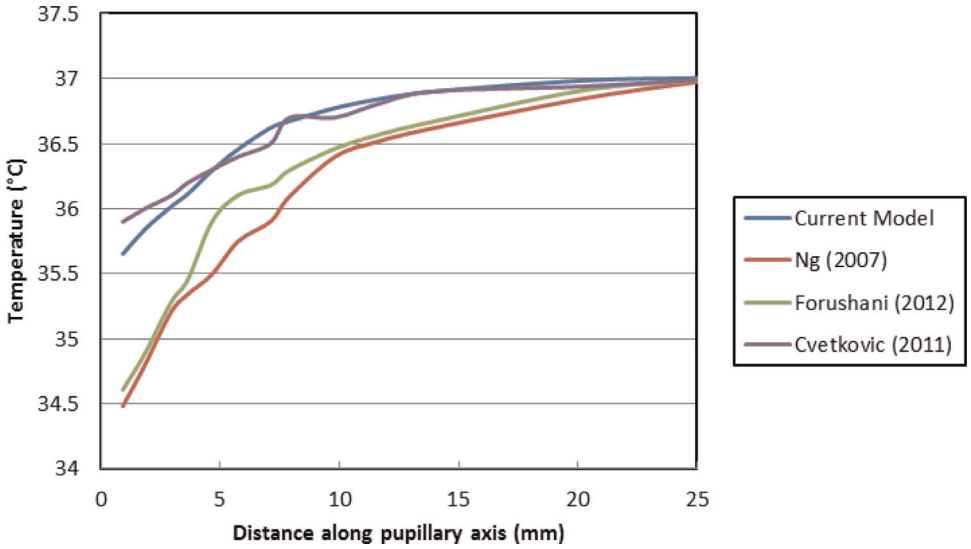

Fig. 7. Comparison of the temperature distribution for ambient temperature 25 °C with values from other models.

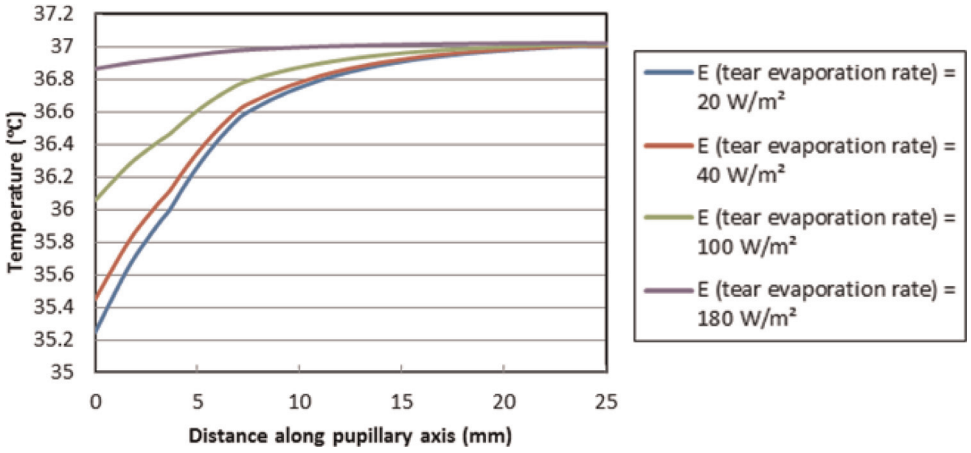

Fig. 8. Temperature distribution under steady condition for four different tear evaporation rates (20, 40, 100 and 180 W/m^2) along pupillary axis.

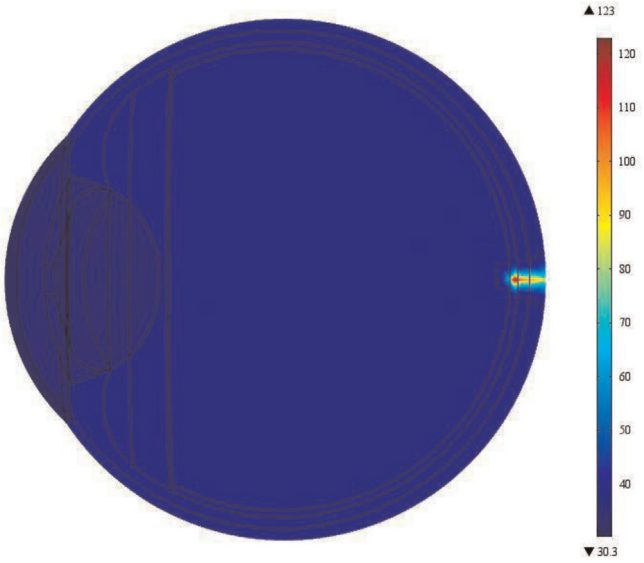

Fig. 9. Transient-state temperature distribution in human eye under Nd:Yag laser radiation.

temperature variations of six optional points as functions of time.

Argon laser: LASIK or surgery of cornea is one of the applications of this laser. The results show high temperature increase in frontal part of the eye, particularly inside the cornea. This is a precious finding, since this type of laser is used specially for corneal surgery with photoablation process.

Fig. 15 shows the temperature distribution inside the eye after applying this laser. The temperature variations of six optional points can be seen in Fig. 16

5. Discussion

5.1. Steady state condition results

In this case, there has not been any trace of the laser and temperature distribution under steady conditions is presented. As can be seen, the highest temperatures are inside the distal regions of the eye (retina, sclera, vitreous humour and choroid), while frontal regions (cornea and iris) have got lower temperatures. It is worth mentioning that these results are in good agreement with those of previous works (Ng and Ooi, 2006; Cvetkovic et al. 2011; Forushani et al., 2012) (Fig. 7).

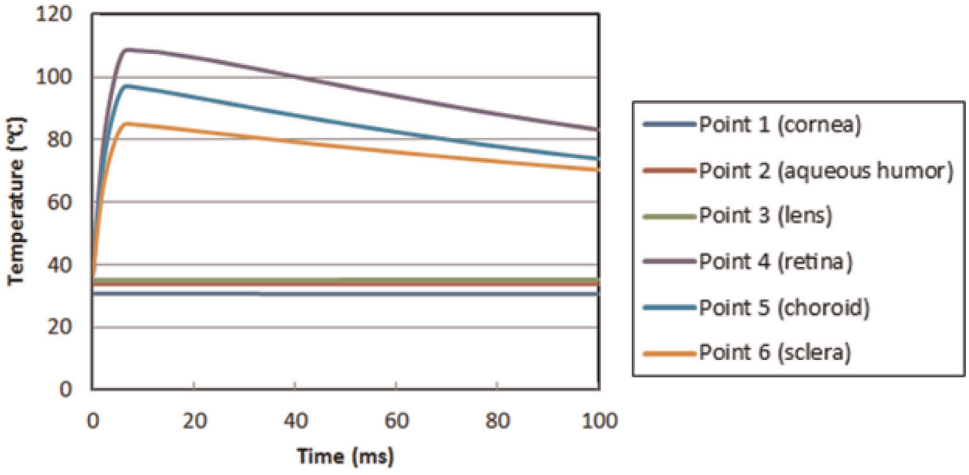

Fig. 10. Temperature variations of optional points (cornea, aqueous humour, lens, retina, choroid, sclera) after applying Nd:Yag laser radiation.

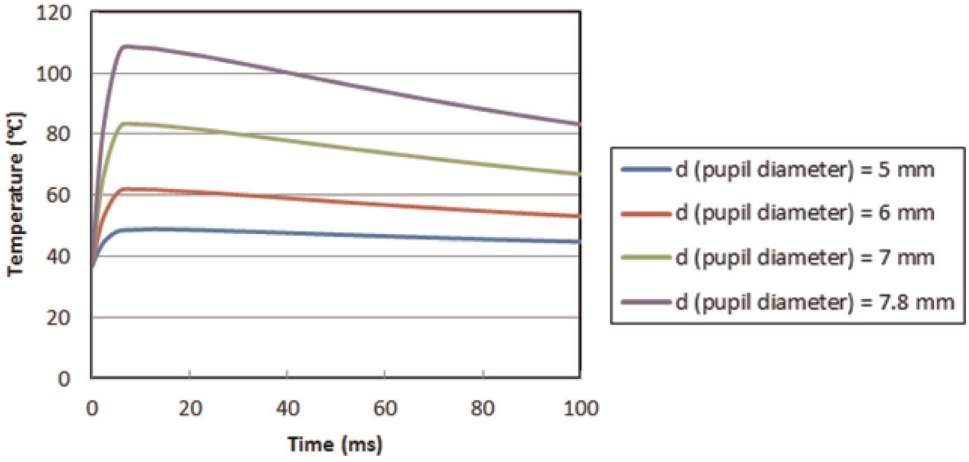

Fig. 11. The effect of the variation of the pupil diameter (5, 6, 7 and 7.8 mm) on point No. 4 (retina).

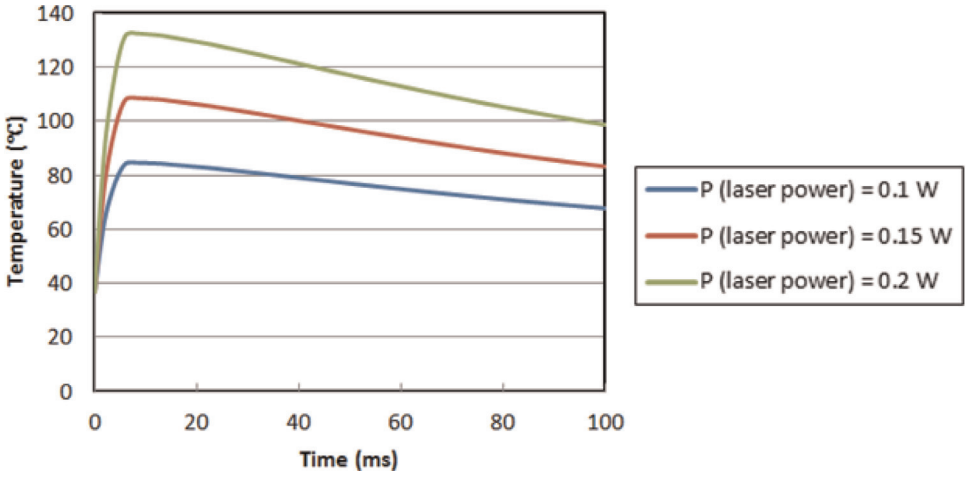

Fig. 12. The effect of the variation of the laser power (0,1, 0,15 and 0.2 W) on point No. 4 (retina).

5.2. *Transient condition results*

Nd:Yag laser: This laser is mostly used for the surgery of the distal regions of the eye like sclera and retina. Nd:Yag laser is applied for retinal photocoagulation, retinotomy for internal drainage of subretinal fluid and transscleral retinal photocoagulation. The wavelength of this laser is 1064 nm and has been applied for 10 ms. In Fig. 9, As seen and as we expected, the maximum temperature occurs in retina (110 °C). Moreover, sclera and choroid regions have relatively high temperatures, though with more limited domains. On the other hand, the other regions are exposed to temperatures lower than 40 °C which are crystal clear in Figs. 9 and 10. Another important fact to be fully taken into account is that the temperature of the retina is increased with increasing the exposure time and this increase is not ceased until switching off the laser. By the moment the laser is turned off, the

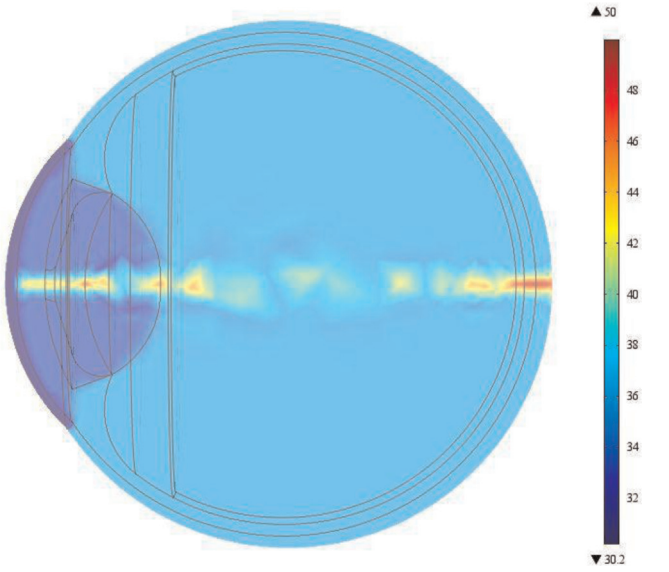

Fig. 13. Transient-state temperature distribution in human eye under Nd:Yap laser radiation.

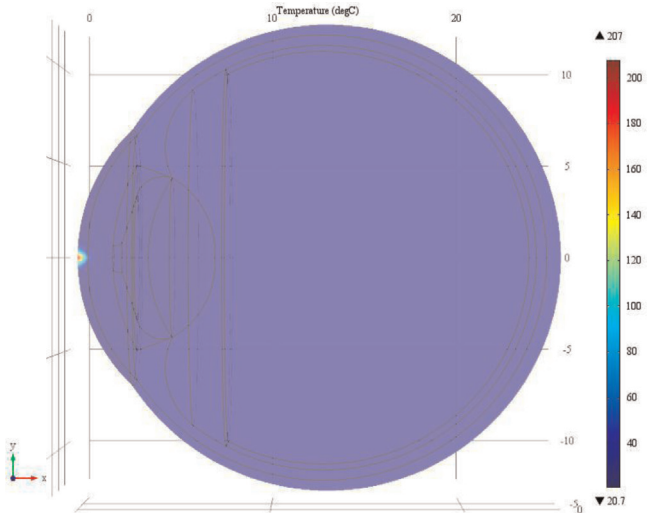

Fig. 15. Transient-state temperature distribution in human eye under Argon laser radiation.

temperature decreases with high speed which is due to blood perfusion. The pupil diameter ranges from 5 to 7.8 mm which is influenced by the amount of the environmental light. The maximum temperature that occurs inside the eye increases with the increasing of the laser power and the pupil diameter.

The results of this laser simulation are in decent agreement with the results of Narasimhan and Jha (2012) and Cvetković et al. (2008). It is also important to mention that the maximum temperature causes significant damage to the eye tissue.

Nd:Yap laser: This laser is most commonly used in retinal surgery. The wavelength of this laser is 1340 nm and has been applied for 1 ms. The maximum temperature of 49 °C occurs in retina and partially in aqueous humour and lens. The temperature of the centreline of the eye is increased with increasing the exposure time and this increase continues until the laser is turned off.

The difference between this laser and the two other lasers is the uniform temperature distribution along the centreline of the eye, which is due to the equivalence of absorption coefficients of aqueous humour and iris for this laser (Table 2). The results of this laser simulation are in decent agreement with the results of Mirnezami et al. (2013).

Argon laser: LASIK or surgery of cornea is one of the applications of this laser. The results show high temperature increase in frontal part of the eye, particularly inside the cornea. This is a precious finding, since this type of laser is used specially for corneal surgery with photoablation process.

The wavelength of this laser is 193 nm and has been applied for 100 ns. The maximum temperature occurs in cornea which is equal to 207 °C which has a good agreement with the calculated temperature in Cvetković et al. (2008).

Our results support the fact that Lens acts as an optical filter for UV radiations. While the temperature of the cornea rises rapidly, Lens prevents the temperature rise of the dorsal areas of the eye. This increasing of temperature has got another reason that is the high absorption coefficient of cornea which absorbs almost all UV radiation.

After applying this laser, no significant temperature changes are seen in other parts of the eye.

6. Conclusions

In this paper, numerical simulations have been conducted to evaluate the effects of three different lasers namely Nd:Yag, Nd:Yap and Argon with wavelengths of respectively 1340, 1064 and 193 nm on the human eye. The maximum temperature under Nd:Yag laser equals to 110 °C which occurs in retina. On the other hand, the maximum temperatures under Nd:Yap and Argon lasers are 49 °C and

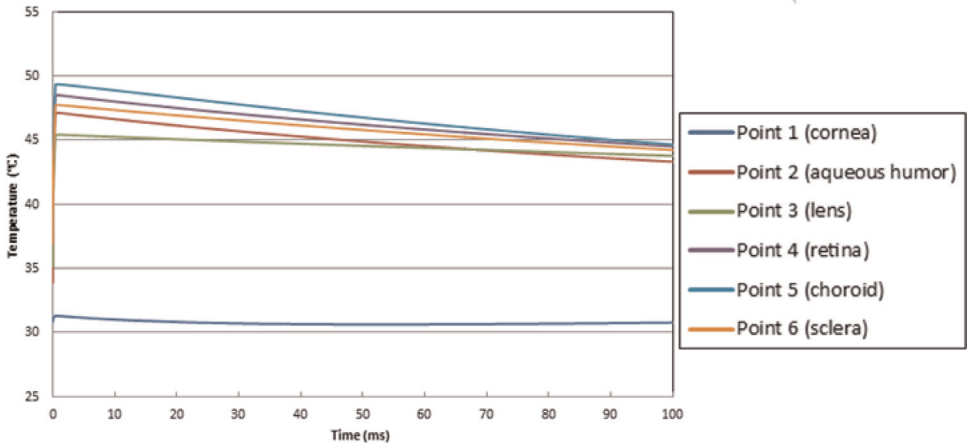

Fig. 14. Temperature variations of optional points (cornea, aqueous humour, lens, retina, choroid, sclera) after applying Nd:Yap laser radiation.

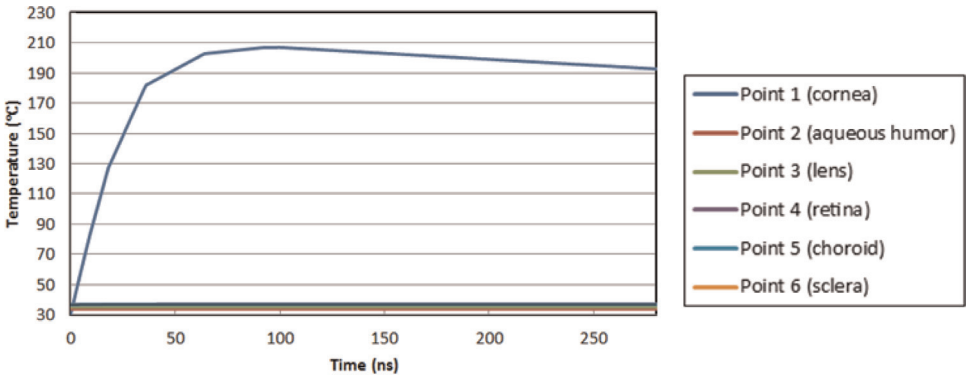

Fig. 16. Temperature variations of optional points (cornea, aqueous humour, lens, retina, choroid, sclera) after applying Argon laser radiation.

207 °C which occurs in retina and cornea, respectively. Furthermore, the effects of power of laser and the diameter of pupil have also been studied which have dramatic impact on the temperature of retina. In addition, as in this model, unlike the earlier studies, most of the determinant factors in bioheat transfer analysis such as blood perfusions of different regions of the eye tissue have been taken into account, the authors believe that this procedure is a reliable method for determining the maximum temperature and temperature distribution in the human eye under different lasers duration of applying each laser. This simulation shows that after switching off the laser, blood perfusion cools down the eye faster.

It should be noted that in this study the fluid characteristics of the aqueous humour of the eye have not been investigated. Therefore, a more careful scrutiny at the boundary conditions of this simulation can be a significant challenge in this field.

References

Chua, K., Ho, J., Chou, S., Islam, M., 2005. On the study of the temperature distribution within a human eye subjected to a laser source. Int. Commun. Heat Mass Transf. 32 (8), 1057–1065.

Cvetković, M., Poljak, D., and Pretta, A., 2008. Analysis of the Temperature Distribution to the Human Eye Exposed to Laser Radiation. s.1, sn.

Cvetković, M., Poljak, D., Pretta, A., 2011. FETD computation of the temperature distribution induced into a human eye by a pulsed laser. Prog. Electromagn. Res. 120, 403–421.

DeMarco, S., Raleigh, N., Lazzi, G., Wentai, L., Weiland, J., Humayun, M., 2003. Computed SAR and thermal elevation in a 0.25-mm 2-D model of the human eye and head in response to an implanted retinal stimulator – Part I: models and methods. IEEE Trans. Antennas Propag. 51 (9), 2274–2285.

Emery, A., Kramar, P., Guy, A., Lin, J., 1975. Microwave induced temperature rises in rabbit eyes in cataract research. J. Heat Transf. 97 (1), 123–128.

Forushani, R., Hassani, K., Izadi, F., 2012. Steady state heat analysis of the eye using finite element method. J. Biomed. Res. 23 (1), 99–104.

Gokul, K., Dil Bahadur, G., Pushpa, R., 2013. FEM approach for transient heat transfer in human eye. Appl. Math. 4 (10), 30–36.

Heussner, N., Holl, L., Nowak, T., Beuth, T., Spitzer, M.S., Stork, W., 2014. Prediction of temperature and damage in an irradiated human eye—utilization of a detailed computer model which includes a vectorial blood stream in the choroid. Comput. Biol. Med. 51, 35–43.

Jelinkova, H., Pasta, J., Sulc, J., Nemec, M., Koranda, P., Hrabal, P., 2004. Near-infrared Nd:YAP laser radiation transmission through the human eye tissue structure. Proc. SPIE, 24; , pp. 53–58.

Lagendijk, J.J.W., 1982. A Mathematical model to calculate temperature distributions in human and rabbit eyes during hyperthermic treatment. Phys. Med. Biol. 27 (11), 1301.

Niemz, M.H., 2007. Laser–Tissue Interactions: Fundamentals and Applications, third ed. Springer, Berlin.

Mirnezami, S., Jafarabadi, M., Abrishimi, M., 2013. Temperature distribution simulation of the human eye exposed to laser radiation. J. Lasers Med. Sci. 4 (4).

Narasimhan, A., Kumar Jha, K., 2012. Bio-heat transfer simulation of retinal laser irradiation. Int. J. Numer. Methods in Biomed. Eng. 28 (5), 547–559.

Narasimhan, A., Jha, K., Gopal, L., 2010. Transient simulations of heat transfer in human eye undergoing laser surgery. Int. J. Heat Mass Transf. 53 (1–3), 482–490.

Ng, E., Ooi, E., 2006. FEM simulation of the eye structure with bioheat analysis. Comput. Methods Progr. Biomed. 82 (3), 268–276.

Ooi, E., Ang, W., Ng, E., 2007. Bioheat transfer in the human eye: a boundary element approach. Eng. Anal. Bound. Elem. 31 (6), 494–500.

Pennes, H., 1948. Analysis of tissue and arterial blood temperatures in the resting human forearm. J. Appl. Physiol. 1 (2), 93–122.

Priebe, L., Cain, C., Welch, A., 1975. Temperature rise required for production of minimal lesions in the Macaca mulatta retina. Am. J. Ophthalmol. 79 (3), 405–413.

Scott, J.A., 1988. A finite element model of heat transport in the human eye. Phys. Med. Biol. 33 (2), 227–241.

Taflove, A., Brodwin, M., 1975. Computation of the electromagnetic fields and induced temperatures within a model of the microwave-irradiated human eye. IEEE Trans. Microwave Theory Tech. 23 (11), 888–896.

Amin Joukar was born in 1990 in Iran. He has studied mechanical engineering in B.Sc level at Yasouj University. At present time he is studying biomedical engineering at Sahand University of Technology. He has published 3 conference papers.

Erfan Nammakie was born in 1986 in Iran. He holds a bachelor's degree in mechanical heat and transfer from Islamic Azad University of Mashhad. He is now studying biomedical engineering at Sahand University of Technology in master level. He has published 1 conference paper and 1 ISI paper.

Dr. Hanieh Niroomand-Oscuii was born in 1974 in Iran. She did the Ph.D in biomedical engineering in Amirkabir University of Technology degree in 2007. She is Associate professor of biomedical engineering since 2014. She teaches heat and mass transfer in biomedical engineering, biofluid mechanics, bioinstrumentation and artificial organs courses in Sahand University of Technology. Her research interests include cardiovascular biomechanics, fluid-solid interaction in biologic systems, heat & mass transport in biological systems and artificial organs. She has published more than 35 conference papers, 15 ISI papers in the fields which are mentioned above.